Light-Emitting Carbazole Derivatives: Potential Electroluminescent Materials

K. R. Justin Thomas,[†] Jiann T. Lin,*[,†,‡] Yu-Tai Tao,*[,†] and Chung-Wen Ko[†]

Contribution from the Institute of Chemistry, Academia Sinica, Taipei, Taiwan 115, Republic of China, and Department of Chemistry, National Central University, Chungli, Taiwan 320, Republic of China

Received March 29, 2001

Abstract: Stable carbazole derivatives that contain peripheral diarylamines at the 3- and 6-positions and an ethyl or aryl substituent at the 9-position of the carbazole moiety have been synthesized via palladium-catalyzed C−N bond formation. These new carbazole compounds (carbs) are amorphous with high glass transition temperatures (T_g, 120−194 °C) and high thermal decomposition temperatures (T_d > 450 °C). The compounds are weakly to moderately luminescent in nature. The emission wavelength ranges from green to blue and is dependent on the substituent at the peripheral nitrogen atoms. Two types of light-emitting diodes were constructed from carb: (I) ITO/carb/TPBI/Mg:Ag and (II) ITO/carb/Alq_3/Mg:Ag, where TPBI and Alq_3 are 1,3,5-tris(*N*-phenylbenzimidazol-2-yl)benzene and tris(8-hydroxyquinoline) aluminum, respectively. In type I devices, the carb functions as the hole-transporting as well as emitting material. In type II devices, either carb, or Alq_3 is the light-emitting material. Several green light-emitting devices exhibit exceptional maximum brightness, and the physical performance appears to be better than those of typical green light-emitting devices of the structure ITO/diamine/Alq_3/Mg:Ag. The relation between the LUMO of the carb and the performance of the light-emitting diode is discussed.

Introduction

Electroluminescent (EL) devices based on organic thin layers have attracted much attention because of the potential application to large-area flat-panel displays and light-emitting diodes (LEDs).[1] Considerable progress has been made on organic LEDs (OLEDs) using both low molecular weight organic materials and polymers. Low molecular weight small molecules can generally be vacuum-deposited as thin films. This deposition technique was first utilized by Tang and VanSlyke[2] to build up multilayered OLEDs. Through proper choice of electron- and hole-transport materials, a better confinement of charge recombination region and, therefore, a better efficiency, can be achieved in a multilayer device. One simple and useful method for the construction of OLEDs employs a bilayer structure comprising a hole-transport layer and an electron-transport layer, with one or both layers being luminescent.[3]

The durability, i.e., thermal and morphological stability of deposited films, is another important factor that has a dramatic influence on the physical performance of organic LEDs.[4] Usually an amorphous film with higher glass transition temperature (T_g) is desired.[5] It is well recognized that the thermal stability or glassy-state durability of organic compounds can be greatly improved upon incorporation of a carbazole[6] moiety in the core structure. Furthermore, the carbazole moiety can be easily functionalized at its 3-, 6-, or 9-positions and covalently linked to other molecular moieties.[7] Therefore, we felt that thermally and morphologically stable molecules possessing dual functions, light emitting and hole transporting, should be available by using carbazole as the central core. No such compounds were reported, even though poly(*N*-vinylcarbazole) (PVK)[8] and some derivatives of carbazole[9] have found applications related to OLEDs. Here we describe the preparation of a series of carbazole compounds with peripheral arylamines. These compounds are green or blue emitting and capable of hole transporting. Results of some of these materials have been communicated.[10]

Experimental Section

General Information. Unless otherwise specified, all the reactions were performed under nitrogen atmosphere using standard Schlenk techniques. Toluene was distilled from sodium and benzophenone under nitrogen atmosphere. Dichloromethane for spectroscopic and electrochemical measurements were distilled from calcium hydride under nitrogen atmosphere. ^1H and ^{13}C NMR spectra were recorded on a Bruker 300-MHz spectrometer operating at 300.135 and 75.469 MHz, respectively. Emission spectra were recorded on a Perkin-Elmer

* Corresponding author. Fax: Int. code +(2)27831237. E-mail: jtlin@chem.sinica.edu.tw.

† Academia Sinica.

‡ National Central University.

(1) (a) Jenekhe, S. A. *Adv. Mater.* **1995**, *7*, 309. (b) Miyata, S., Nalwa, H. S., Eds.; *Organic Electroluminescent Materials and Derivatives*; Gordon and Breach: New York, 1997. (c) Hide, F.; Diaz-Garcia, M. A.; Schartz, B. J.; Heeger, A. J. *Acc. Chem. Res.* **1997**, *30*, 430. (d) Kraft, A.; Grimsdale, A. C.; Holms, A. B. *Angew. Chem., Int. Ed. Engl.* **1998**, *37*, 402.

(2) Tang, C. W.; VanSlyke, S. A. *Appl. Phys. Lett.* **1987**, *51*, 913.

(3) Chen, C. H.; Shi, J.; Tang, C. W. *Coord. Chem. Rev.* **1998**, *171*, 161.

(4) Tokito, S.; Tanaka, H.; Noda, K.; Okada, A.; Taga, T. *Appl. Phys. Lett.* **1997**, *70*, 1929.

(5) (a) Shirota, Y. *J. Mater. Chem.* **2000**, *10*, 1. (b) Naito, K.; Miura, A. *J. Phys. Chem.* **1993**, *97*, 6240.

(6) (a) Kuwabara, Y.; Ogawa, H.; Inada, H.; Noma, N.; Shirota, Y. *Adv. Mater.* **1994**, *6*, 677. (b) Koene, B. E.; Loy, D. E.; Thompson, M. E. *Chem. Mater.* **1998**, *10*, 2235. (c) O'Brien, D. F.; Burrows, P. E.; Forrest, S. R.; Koene, B. E.; Loy, D. E.; Thompson, M. E. *Adv. Mater.* **1998**, *10*, 1108.

(7) Joule, J. A. *Adv. Heterocycl. Chem.* **1984**, *35*, 83.

(8) (a) Zhang, C.; von Seggern, H.; Pakbaz, K.; Kraabel, B.; Schmidt, H. W.; A. J. Heeger, A. J. *Synth. Met.* **1994**, *62*, 35. (b) Hu, B.; Yang, Z.; Karasz, F. E. *J. Appl. Phys.* **1994**, *76*, 2419. (c) Wang, G.; Yuan, C.; Wu, H.; Wei, Y. *J. Appl. Phys.* **1995**, *78*, 2679. (d) Wang, Y. Z.; Epstein, A. J. *Acc. Chem. Res.* **1999**, *32*, 217.

(9) (a) Romero, D. B.; Schaer, M.; Leclerc, M.; Adès, D.; Siove, A.; Zuppiroli, L. *Synth. Met.* **1996**, *80*, 271. (b) Romero, D. B.; Nüesch, F.; Benazzi, T.; Adès, D.; Siove, A.; Zuppiroli, L. *Adv. Mater.* **1997**, *9*, 1158. (c) Maruyama, S.; Tao, X.-T.; Hokari, H.; Noh, T.; Zhang, Y.; Wada, T.; Sasabe, H.; Suzuki, H.; Watanabe, T.; Miyata, S. *J. Mater. Chem.* **1999**, *9*, 893. (d) Zhu, Z.; Moore, J. S. *J. Org. Chem.* **2000**, *65*, 116.

(10) Preliminary results were previously communicated: Justin Thomas, K. R.; Lin, J. T.; Tao, Y.-T.; Ko, C.-W. *Adv. Mater.* **2000**, *12*, 1949.

10.1021/ja010819s CCC: $20.00
Published on Web 08/28/2001

Scheme 1

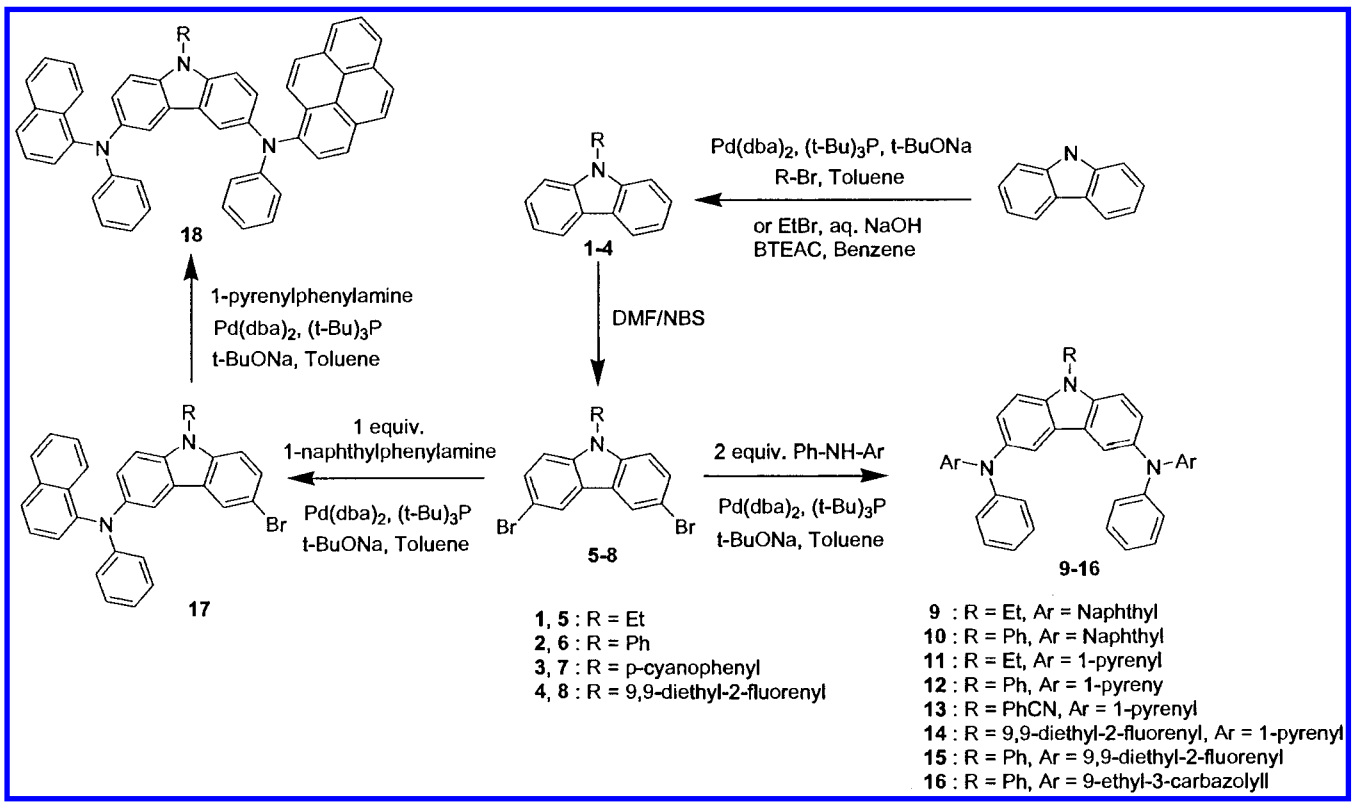

spectrofluorometer, and the quantum efficiencies were obtained by standard method using Coumarin I ($\Phi_f = 0.99$ in EA) as reference. All chromatographic separations were carried out on silica gel (60M, 230−400 mesh). Cyclic voltammetry experiments were performed with a BAS-100 electrochemical analyzer. All measurements were carried out at room temperature with a conventional three-electrode configuration consisting of a platinum working electrode, an auxiliary platinum electrode, and a nonaqueous $Ag/AgNO_3$ reference electrode. The solvent in all experiments was CH_2Cl_2, and the supporting electrolyte was 0.1 M tetrabutylammonium hexafluorophosphate. The $E_{1/2}$ values were determined as $^1/_2(E_p^a + E_p^c)$, where E_p^a and E_p^c are the anodic and cathodic peak potentials, respectively. All potentials reported are referenced to Fc^+/Fc external standard (+0.250 V relative to the $Ag/AgNO_3$ electrode) and are not corrected for the junction potential. DSC measurements were carried out using a Perkin-Elmer 7 series thermal analyzer at a heating rate of 10 °C/min. TGA measurements were performed on a Perkin-Elmer TGA7 thermal analyzer. Mass spectra (FAB) were recorded on a VG70-250S mass spectrometer. Elementary analyses were performed on a Perkin-Elmer 2400 CHN analyzer. *N*-Phenyl-1-naphthylamine and $Pd(dba)_2$ were obtained from commercial sources and used as received. 3,6-Dibromo-9-ethylcarbazole,[11] *N*-pyrenylphenylamine,[10] 3,6-dibromo-9-phenylcarbazole,[11] and 9-(*p*-cyanophenyl)carbazole[12] were synthesized by following literature procedures.

General Procedure for the Synthesis of Carbazolylamines. The corresponding N-substituted-3,6-dibromocarbazole (**5**−**8**) (1.0 mmol), a secondary amine (2.1 mmol), $Pd(dba)_2$ (0.022 g, 0.04 mmol), $(t\text{-Bu})_3P$ (0.008−0.012 g, 0.04−0.06 mmol), sodium *tert*-butoxide (0.288 g, 3.0 mmol), and toluene (20 mL) were mixed together and heated at 80 °C for 4−6 h. The reaction was quenched with water (30 mL) and the organic layer taken into 100 mL of diethyl ether, washed with brine solution, and dried over $MgSO_4$. Evaporation of the solvent under vacuum resulted in a yellow residue. The residue was adsorbed in silica gel and purified by column chromatography using a dichloromethane/hexane mixture as eluent.

Compounds 9-ethyl-*N*,*N*′-dinaphthalen-1-yl-*N*,*N*′-diphenyl-9*H*-carbazole-3,6-diamine (**9**), *N*,*N*′-dinaphthalen-1-yl-9-*N*,*N*′-triphenyl-9*H*-carbazole-3,6-diamine (**10**), 9-ethyl-*N*,*N*′-diphenyl-*N*,*N*′-dipyren-1-yl-9*H*-carbazole-3,6-diamine (**11**), *N*,*N*′-dipyren-1-yl-9,*N*,*N*′-triphenyl-9*H*-carbazole-3,6-diamine (**12**), 4-[3,6-bis(phenylpyren-1-yl-amino)carbazol-9-yl]benzonitrile (**13**), 9-(9,9-diethylfluoren-2-yl)-*N*,*N*′-diphenyl-*N*,*N*′-dipyren-1-yl-9*H*-carbazole-3,6-diamine (**14**), *N*,*N*′-bis(9,9-diethyl-9*H*-fluoren-2-yl)-9-*N*,*N*′-triphenyl-9*H*-carbazole-3,6-diamine (**15**), *N*,*N*′-bis(9-ethyl-9*H*-carbazol-3-yl)-9-*N*,*N*′-triphenyl-9*H*-carbazole-3,6-diamine (**16**), (6-bromo-9-ethyl-9*H*-carbazol-3-yl)naphthalen-1-ylphenylamine (**17**), 9-ethyl-*N*-naphthalen-1-yl-*N*,*N*′-diphenyl-*N*′-pyren-1-yl-9*H*-carbazole-3,6-diamine (**18**), 9-phenyl-*N*,*N*′-dipyren-1-yl-*N*,*N*′-di-*p*-tolyl-9*H*-carbazole-3,6-diamine (**19**), and *N*,*N*′-bis(4-methoxyphenyl)-9-phenyl-*N*,*N*′-dipyren-1-yl-9*H*-carbazole-3,6-diamine (**20**) were synthesized by similar procedures, and only the preparation of **15** will be described in detail. The synthesis and characterization of **12**, **19**, and **20** were provided in our earlier publication.[10] Those data for other compounds are deposited as Supporting Information.

***N*,*N*′-Bis(9,9-diethyl-9*H*-fluoren-2-yl)-9,*N*,*N*′-triphenyl-9*H*-carbazole-3,6-diamine (15).** Aniline (1.12 g, 12 mmol), 2-bromo-9,9-diethyl-9*H*-fluorene (3.01 g, 10 mmol), sodium *tert*-butoxide (1.44 g, 15 mmol), $Pd(dba)_2$ (0.11 g, 0.2 mmol), tri(*tert*-butyl)phosphine (0.04−0.06 g, 0.2−0.3 mmol), and toluene (20 mL) were stirred together and heated at 80 °C for 3 h. After cooling, it was quenched with water and extracted with diethyl ether (3 × 50 mL). The combined ethereal extract was washed with brine solution and dried over anhydrous $MgSO_4$. Evaporation of volatiles left a colorless syrup, which on column chromatography produced (9,9-diethyl-9*H*-fluoren-2-yl)-phenylamine in 81% yield as a colorless solid: MS (EI) *m*/*e* 313 (M^+); ^{1}H NMR (acetone-d_6) δ 7.65 (d, J = 7.9 Hz, 2 H), 7.33 (br, s, 1 H), 7.28−7.13 (m, 9 H), 6.85 (t, J = 7.4 Hz, 1 H), 2.04 (m, 4 H), 0.28 (t, J = 7.3 Hz, 6 H). Anal. Calcd for $C_{23}H_{23}N$: C, 88.13; H, 7.40; N, 4.47. Found: C, 88.01; H, 7.45; N, 4.39. Coupling of (9,9-diethyl-9*H*-fluoren-2-yl)phenylamine with **6** yielded **15**, which was isolated as pale yellow solid in 88% yield: MS (FAB) *m*/*e* 865.5 (M^+); ^{1}H NMR (acetone-d_6) δ 7.86 (d, J = 2.0 Hz, 2 H), 7.70−7.60 (m, 8 H), 7.56−7.52 (m, 1 H), 7.40 (d, J = 8.5 Hz, 2 H), 7.28−7.15 (m, 14 H), 7.06 (d, J = 8.5 Hz, 4 H), 6.98−6.89 (m, 4 H), 1.90 (m, 8 H). Anal. Calcd for $C_{64}H_{55}N_3$: C, 88.75; H, 6.40; N, 4.85. Found: C, 88.69; H, 6.43; N, 4.73.

LEDs Fabrication and Measurement. Electron-transporting materials 1,3,5-tris(*N*-phenylbezimidazol-2-yl)benzene (TPBI) and tris(8-hydroxyquinolinealuminum) (Alq_3) were synthesized according to

(11) Park, M.; Buck, J. R.; Rizzo, C. J. *Tetrahedron* **1998**, *54*, 12707.
(12) Mann, G.; Hartwig, J. F.; Driver, M. S.; Fernández-Rivas, C. *J. Am. Chem. Soc.* **1998**, *120*, 827.

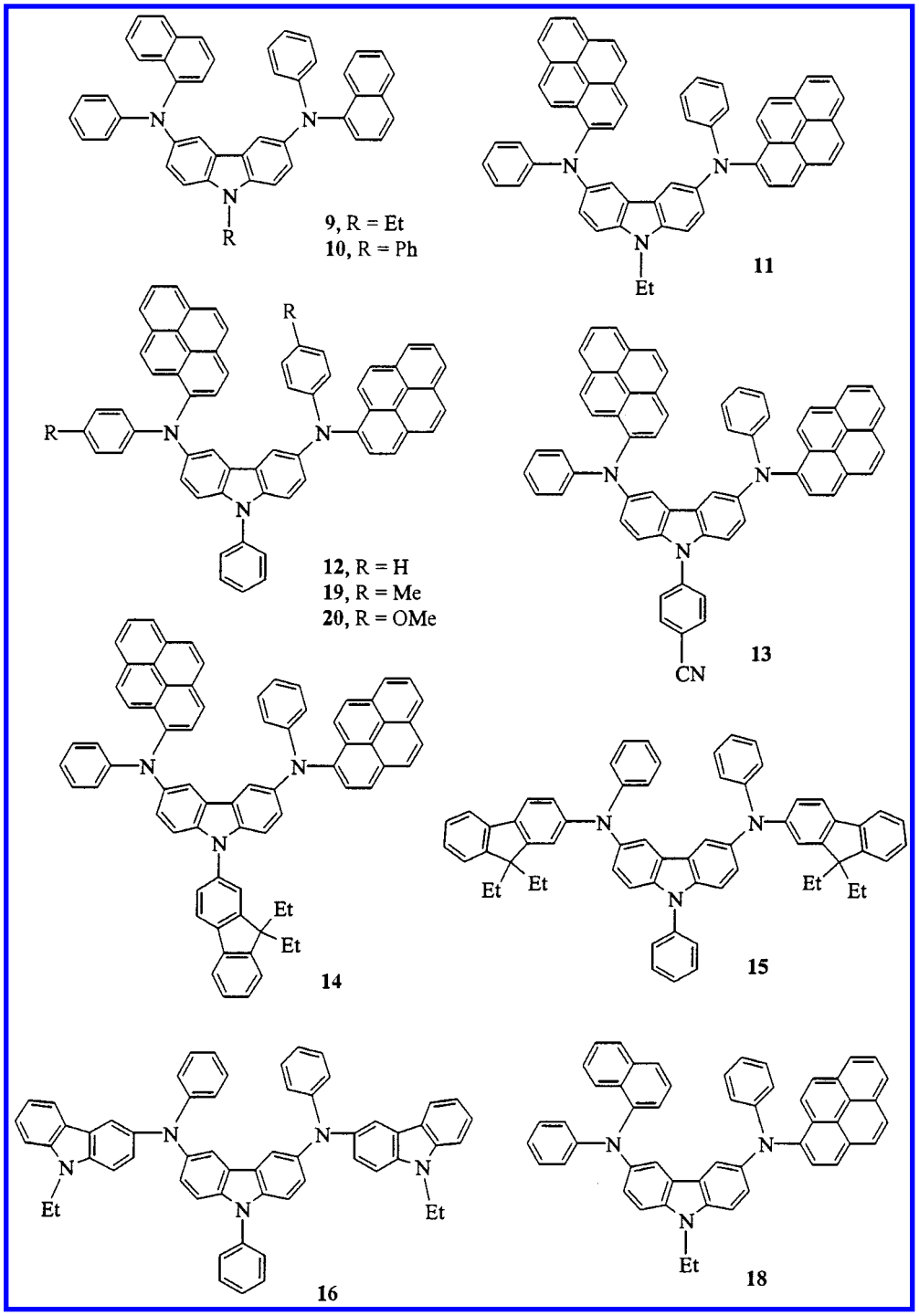

Figure 1. Structure of the carbazole compounds.

literature procedures[3,13] and were sublimed twice prior to use. Prepatterned ITO substrates with an effective individual device area of 3.14 mm^2 were cleaned as described in a previous report.[14] Double-layer EL devices using carbazole derivatives as the hole-transport layer and TPBI or Alq_3 as the electron-transport layer were fabricated. For comparison, a typical device using 1,4-bis(1-naphthylphenylamino)-biphenyl (NPD) as the hole-transport layer was also prepared. All devices were prepared by vacuum deposition of 400 Å of the hole-transporting layer, followed by 400 Å of TPBI or Alq. An alloy of magnesium and silver (~10:1, 500 Å) was deposited as the cathode, which was capped with 1000 Å of silver. The $I-V$ curve was measured on a Keithley 2400 source meter in ambient environment. Light intensity was measured with a Newport 1835 optical meter.

Results and Discussion

Synthesis of Carbazole-3,6-diamines. Scheme 1 outlines the synthesis of all compounds used in this study. The structures of new carbazole-3,6-diamines are illustrated in Figure 1. Arylamines can be obtained either by the copper-catalyzed Ullmann condensation[15] or palladium-catalyzed cross-coupling reactions.[16] Ullmann reactions involve rather high temperatures and prolonged reaction times and are limited to aryl iodides. Often low yields and homocoupled side products diminish the utility of these reactions in broader sense. However, the advent

(13) (a) Shi, J.; Tang, C. W.; Chen, C. H. U.S. Patent, 5,645,948, 1997. (b) Sonsale, A. Y.; Gopinathan, S.; Gopinathan, C. *Indian J. Chem.* **1976**, *14*, 408.

(14) Balasubramaniam, E.; Tao, Y. T.; Danel, A.; Tomasik, P. *Chem. Mater.* **2000**, *12*, 2788.

Table 1. Physical Data for the Compounds

compd	T_g/T_m,[a] °C	T_d,[b] °C	λ_{max} (ϵ_{max}, 10^{-3} M^{-1} cm^{-1}),[c] nm	λ_{em} (Φ_f),[d] nm	λ_{em},,[e] nm	E_{ox} (ΔE_p),[f] mV	HOMO/LUMO,[g] eV
9	120/na	490	351 (19.0), 278 (52.2), 257 (47.3)	497 (0.05)	463	127 (78), 518 (76), 1164 (i)	4.93/2.00
10	123/na	509	351 (18.4), 306 (41.9), 271 (47.6)	486 (0.07)	454	189 (68), 538 (75), 1145 (i)	4.99/2.07
11	174/na	510	408 (21.2), 328 (51.1), 274 (63.2)	548 (0.03)	523	116 (63), 448 (74), 1012 (i)	4.91/2.33
12	180/355	463	408 (21.0), 318 (55.0), 274 (61.3)	539 (0.12)	512	167 (74), 457 (69), 1002 (i)	4.97/2.21
13	194/na	555	385 (40.0), 318 (68.3), 173 (94.1)	515 (0.18)	509	241 (84), 469 (74), 997 (i)	5.04/2.40
14	185/na	621	406 (33.3), 320 (83.8), 275 (104.0)	537 (0.08)	511	159 (87), 455 (78), 1018 (i)	4.96/2.35
15	132/na	566	352 (62.7), 326 (61.6)	439 (0.08)	461	125 (76), 394 (75), 932 (63), 1219 (i)	4.92/1.86
16	152/na	532	309 (88.8), 286 (87.0)	450 (0.12)	469	17 (72), 191 (73), 637 (73), 745 (70)	4.82/1.86
18	174/na	554	383 (16.7), 316 (47.5), 274 (62.9)	548 (0.05)	519	115 (72), 477 (76), 1071 (i)	4.92/2.22
19	184/na	513	415 (26.6), 319 (71.7), 274 (78.1)	543 (0.11)	529	111 (71), 511 (73), 818 (76), 986 (i)	4.91/2.24
20	183/na	455	420 (23.7), 319 (64.2), 274 (71.0)	553 (0.19)	541	63 (77), 348 (72), 769 (63), 885 (75)	4.86/2.24
TPD	60/175	382	311, 353			314 (68)	
NPD	100/265	479	271, 342			342 (66)	
ITO							4.70 (E_F)/na
TPBI						1.80	6.20/2.70
Alq_3							6.09/2.95
Mg:Ag							na/3.70 (E_F)

[a] Obtained from DSC measurements; na, T_m not detected. [b] Obtained from TGA measurements. [c] Measured in CH_2Cl_2 solution. [d] Measured in CH_2Cl_2 solution; Φ_f: fluorescence quantum efficiency. [e] Film samples. [f] Measured in CH_2Cl_2. All E_{ox} data are reported relative to ferrocene, which has an E_{ox} at 226 mV relative to Ag/Ag^+ and the anodic peak-cathodic peak separation (ΔE_p) is 90 mV; i , irreversible process. The concentration of the complexes used in this experiment was 2.5×10^{-4} M and the scan rate was 100 mV s^{-1}. [g] na, not available.

of palladium-catalyzed N-arylation reactions has opened up the possibility of producing a wide variety of arylamines. Such N-arylations have been successfully achieved with the use of $Pd(OAc)_2/(t\text{-}Bu)_3P$, $Pd(OAc)_2$/DPPF, or $Pd(dba)_2/(t\text{-}Bu)_3P$ (dba = dibenzylideneacetone) as the catalyst combinations in the presence of sodium *tert*-butoxide. Hartwig and co-workers have found that the latter catalyst reduces the reaction time and temperature substantially and improves the yield of C−N coupling product.[16b,c] For the preparation of the 3,6-diaminocarbazoles in this study, we screened all the above three catalysts and found that they worked equally well. However, the use of $Pd(dba)_2/(t\text{-}Bu)_3P$ catalyst[16b,c,17] significantly reduces the reaction time and temperature. As much as 95% isolated yields based on 3,6-dibromocarbazoles could be achieved in these reactions. Such palladium-catalyzed amination reactions at the 3,6-positions of carbazoles have not yet been reported, even though nickel-catalyzed Grignard coupling reactions[18] and Sogonashira coupling reactions[19] of 3,6-dibromocarbazoles have been realized. The incorporation of an aromatic ring at the central nitrogen atom of the carbazole molecule was also effectively catalyzed by $Pd(dba)_2/(t\text{-}Bu)_3P$. The desired 3,6-dibromocarbazoles can be readily synthesized from the reaction of the corresponding carbazoles with 2 equiv of NBS in dimethylformamide.

Preparation of pyrene- and naphthalene-containing unsymmetric diamine **18** was achieved by sequential amination of **6** and the monosubstituted intermediate **17**. **17** was isolated in 45% yield in a 1:1 reaction between 3,6-dibromo-9-ethylcarbazole (**6**) and *N*-(1-naphthyl)phenylamine. This unsymmetric diamine **18** was designed mainly to uncover the role of pyrene in this series of hole-transporting materials. A variation of the *N*-substituent (9-substituent), from ethyl to phenyl or fused aromatics (fluorene), was also introduced in these carbazoles to evaluate the role of N-substituent on tuning the hole-transporting and emitting properties.

Thermal Properties. The thermal properties of the new carbazole compounds were determined by DSC and DTA measurements (Table 1). Except for **12**, all the compounds exhibited a glass transition in the first heating cycle and no melting endotherms and crystallization exotherms were noticed. In the case of **12**, a melting isotherm was observed during the first heating cycle, but rapid cooling led to the formation of a glassy state, which persisted in the subsequent heating cycles. The glass transition temperatures (T_g) of these compounds appear to be rather high among commonly used hole-transport materials, such as 1,4-bis(1-naphthylphenylamino)-biphenyl (α-NPD, T_g = 100 °C) and 1,4-bis(phenyl-*m*-tolylamino)biphenyl (TPD, T_g = 60 °C),[6b] and many starburst arylamines.[5a]

The nonplanar and star-shaped nature of the carbazole compounds may be responsible for easy glass formation. Replacement of a diphenylamino group by a rigid carbazolyl group was found to result in a dramatic increase in the glass transition temperature of triphenylamine-based starburst compounds.[5a] For the carbazole compounds in this study, the role of carbazole in raising T_g is evident when comparing **9** (120 °C) and **10** (123 °C) with NPD (100 °C) or **16** (152 °C) with **9** and **10**. The glass transition temperatures (T_g) of the pyrene-incorporated amines **11**−**14** and **18**−**20** range from 174 to 194 °C, more than 50 °C higher than those of naphthylamine-substituted carbazoles **9** and **10**, which are 120 and 123 °C, respectively. The role of pyrene in raising T_g is clearly demonstrated from the steep rise of T_g in going from **9** (120 °C) to **11** (174 °C) or from **10** (123 °C) to **18** (174 °C) and **12** (180 °C). Apparently bulkier pyrene substituents hamper the intramolecular rotations of the molecules. With the same peripheral substituent diarylamine, replacement of *N*-ethyl substituent by an N-aryl group leads to a small enhancement in the thermal stabilities (**9** → **10** and **11** → **12**). However, the *p*-cyanophenyl group excerts a larger effect (**12** → **13**). This increase in glass transition temperature may be attributed to the polar nature of the cyano moiety.[20] The vapor-deposited film of **11** (T_g = 174 °C) was subjected to heating at 150 °C and scrutinized by polarized microscope periodically. The film remained amorphous even after 20 h. Similar treatment on NPD film ($T_g \sim 100$ °C, $T_c \sim 200$ °C) led to crystallization within 3 h. Such an outcome further points to the correlation between a high T_g and temporal stability of the film. This should be beneficial to the devices' performance.

(15) (a) Aalten, H. L.; van Koten, G.; Grove, D. M. *Tetrahedron* **1989**, *45*, 5565. (b) Paine, A. J. *J. Am. Chem. Soc.* **1987**, *109*, 1496. (c) Lindley, L. *Tetrahedron* **1984**, *40*, 1433. (d) Weingarten, H. *J. Org. Chem.* **1964**, *29*, 977.

(16) (a) Wolfe, J. P.; Wagaw, S.; Marcoux, J.-F.; Buchwald, S. L. *Acc. Chem. Res.* **1998**, *31*, 805. (b) Hartwig, J. F. *Angew. Chem., Int. Ed. Engl.* **1998**, *37*, 2047. (c) Hartwig, J. F. *Synlett* **1997**, 329.

(17) Nishiyama, M.; Yamamoto, T.; Koie, Y. *Tetrahedron Lett.* **1998**, *39*, 617.

(18) Park, M.; Buck, J. R.; Rizzo, C. J. *Tetrahedron* **1998**, *54*, 12707.

(19) Campbell, I. B. In *Organocopper Reagents*; Taylor, R. J. K., Ed.; Oxford University Press: Oxford, U.K., 1994; Chapter 10.

(20) Wang, S.; Oldham, Jr.; W. J.; Hudack, Jr.; R. A.; Bazan, G. C. *J. Am. Chem. Soc.* **2000**, *122*, 5695.

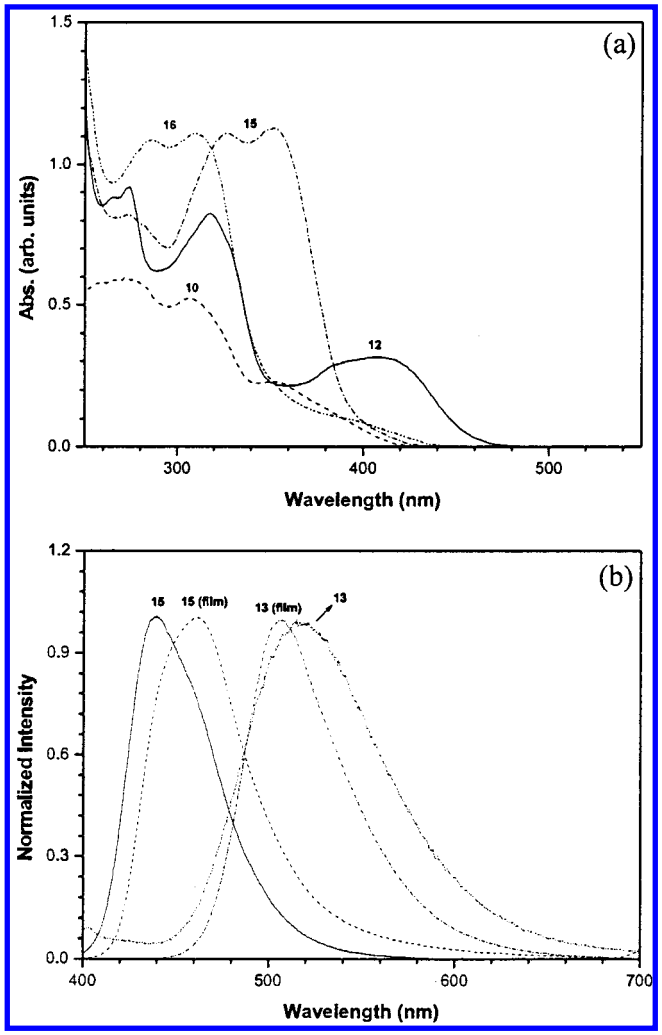

Figure 2. (a) Absorption spectra of the compounds **10**, **12**, **15**, and **16**. (b) Solution (CH_2Cl_2) and film emission spectra of **13** and **15**.

Optical Properties. The absorption and luminescence spectra of the compounds were measured in CH_2Cl_2, and the pertinent data are presented in Table 1. The absorption spectra of the compounds are complex with multiple overlapping broad bands. Some representative spectra are shown in Figure 2a. In general, they display absorptions resulting from the combination of carbazole and pyrene, naphthalene, or fluorene chromophores and cover the entire UV−visible region (250−450 nm). Pyrene-containing compounds display a distinct absorption at the longer wavelength, which may be assigned to localized pyrene $\pi \rightarrow \pi^*$ transition. These diamines are weakly to moderately photoluminescent with emission wavelengths ranging from green to blue. Among the compounds with 3,6-diarylamine substituents, those containing a pyrene moiety (**11**−**14**, **18**−**20**) emit green light ($\lambda_{em} > 515$ nm) in CH_2Cl_2 solution, while a prominent blue shift in luminescent spectra is observed when both pyrenes are replaced by naphthalene (**9** and **10**, $\Delta\lambda = \sim 20-30$ nm), fluorene (**15**; $\Delta\lambda = 100$ nm), or carbazole (**16**; $\Delta\lambda = 89$ nm). In the film state, all the compounds except **15** (Figure 2b) and **16** exhibit a significant blue shift in their emission and bandwidth narrowing. Compounds **15** and **16** may have close packing of the molecules in the film state, and such intermolecular interaction usually raises the ground-state energy of the molecule. On the contrary, the sterically demanding bulky naphthyl and pyrenyl substituents prevent the close packing in the solid state. Studies with solvents of different polarity also confirmed that the red shift in solution (CH_2Cl_2) PL relative to the solid film is mainly due to the solvent effect.

The lowest unoccupied molecular orbital/highest occupied molecular orbital (LUMO/HOMO) energy gaps for the compounds were estimated from the absorption edge of optical absorption spectra.[21] The LUMO levels in these amines are sensitive to the nature of the N-substituents at the 3- and 6-position. The pyrene-containing amines possess a low LUMO/HOMO energy gap when compared to the naphthalene analogues. MO calculations showed that the LUMOs in these molecules are localized mainly on the pyrene (**11**−**14**, **18**−**20**), naphthylene (**9**, **10**), and central carbazole (**15**, **16**), respectively.[22] This is in agreement with the order of LUMO energies, (**11**−**14**, **18**−**20**) < (**9**, **10**) < (**15**, **16**). This order affects the ultimate EL behavior in a device (vide infra).

Cyclic Voltammetric Studies. The electrochemical properties of the compounds were studied by cyclic and differential pulse voltammetric methods, and the redox potentials of the compounds are compiled in Table 1. All the amines display two reversible oxidation waves at relatively low oxidation potentials attributable to the oxidation of the peripheral amines at the 3- and 6-positions of the carbazole core. The first oxidation potential (E_{ox}^1) is subject to the electronic effects of the substituents at the peripheral nitrogen atoms. For instance, the E_{ox}^1 is ordered **12** > **19** > **20**, in accordance with the electron-donating ability of substituents at the para position of the phenyl group. Similarly, E_{ox}^1 is strongly influenced by the carbazole N-substituents. Thus, E_{ox}^1 shifts cathodically in the following order: **11** < **14** < **12** < **13**. Apparently, the electron-donating ethyl group lowers the first oxidation potential in **11**. On the contrary, the electron-withdrawing *p*-cyanophenyl moiety in **13** significantly shifts the first oxidation potential anodically. Stabilization of the cation radicals by electron-donating substituents at a distant conjugation is well documented, particularly when the moieties involved are in communication.[6b,23]

The third oxidation appearing at significantly higher potential than the first two is ascribed to the carbazole core.[24] It is irreversible in all amines with the exception of **15**, **16**, and **20**. In amines **16** and **20**, four reversible redox waves were located, of which the first two originate from the 3,6-substituted amines and the third stems from the carbazole core. The fourth wave may be due to the formation of a dication radical at one of the peripheral amine centers or peripheral carbazole oxidation in **16**. Such a formation is facilitated by the presence of relatively strong electron-donating methoxy substituents or carbazolyl side groups.

Electroluminescent Properties. The HOMO and LUMO energy levels of the materials are very crucial parameters for LED configuration. The HOMO energy levels of the carbazole compounds (Table 1) were calculated from cyclic voltammetry (vide supra) and by comparison with ferrocene (4.8 eV).[25] These together with the absorption spectra were then used to obtain the LUMO energy levels (Table 1).[6b,26] Therefore, the HOMO energy levels (4.86−5.04 eV) of the carbazole compounds (carbs) lie between those of ITO (HOMO, 4.70 eV) and TPBI

(21) Janietz, S.; Bradley, D. D. C.; Grell, M.; Giebeler, C.; Inbasekaran, M.; Woo, E. P. *Appl. Phys. Lett.* **1998**, *73*, 2453.

(22) The molecular orbital calculation (AM1, PC Spartan Pro Ver 1) indicated that the N-substituent (pyrene (**11**−**14**, **18**−**20**), naphthylene (**9**, **10**), fluorene (**15**), and carbazole (**16**)) at the 3- or 6-position is the major component of the LUMOs in the carbazole compounds.

(23) (a) Bellmann, E.; Shaheen, S. E.; Grubbs, R. H.; Marder, S. R.; Kippelen, B.; Peyghambarian, N. *Chem. Mater.* **1999**, *11*, 399. (b) Michinobu, T.; Takahashi, M.; Tsuchida, E.; Nishide, H. *Chem. Mater.* **1999**, *11*, 1969. (c) Lambert, C.; Nöll, G. *Angew. Chem., Int. Ed. Engl.* **1998**, *37*, 2107. (d) Pfeiffer, S.; Hörhold, H.-H.; Boerner, H.; Nikol, H.; Busselt, W. *Proc. SPIE* **1998**, *3476*, 258.

(24) Dapperheld, S.; Steckhan, E.; Brinkhnvs, K.-H. G.; Esch, T. *Chem. Ber.* **1991**, *124*, 2557.

(25) Pommerehne, J.; Vestweber, H.; Guss, W.; Mahrt, R. F.; Bässler, H.; Porsch, M.; Daub, J. *Adv. Mater.* **1995**, *7*, 551.

(26) Thelakkat, M.; Schmidt, H.-W. *Adv. Mater.* **1998**, *10*, 219.

Table 2. Electroluminescence Data for the Compounds

	TPBI/Alq_3				*TPBI*/Alq_3	TPBI/Alq_3	*TPBI* or Alq_3
compd	turn-on voltage, V	voltage,[a] V	brightness,[a] Cd/m^2	quantum effic,[a] %	power effic,[a] lm/W	λ_{em}, nm	CIE, *x*, *y*
9	2.6/2.3	6.0/6.8	1258/2016	1.05/0.68	*0.65*/0.93	460/514	*0.15*, *0.14*; 0.26, 0.50
10	2.5/2.7	6.0/6.6	692/2774	0.73/0.91	*0.36*/1.32	453/508	*0.15*, *0.11*; 0.26, 0.51
11	2.3/3.3	5.9/7.3	4925/3119	1.66/1.10	*2.72*/1.35	516/516	*0.26*, *0.55*; 0.28, 0.53
12	2.5/3.2	5.5/6.8	3937/2601	1.50/0.97	*2.35*/1.15	498/502	*0.23*, *0.49*; 0.24, 0.49
13	2.6/2.7	5.2/6.2	5362/3882	2.10/1.45	*3.26*/1.96	500/500	*0.22*, *0.47*; 0.23, 0.49
14	2.3/3.3	5.4/7.0	4486/3891	1.70/1.39	*2.61*/1.76	500, 526/502, 528	*0.23*, *0.48*; 0.25, 0.53
15	2.8/2.3	6.1/6.2	507/2443	0.48/0.74	*0.28*/1.23	458/521	*0.15*, *0.12*; 0.30, 0.56
16	2.3/2.7	5.6/6.5	479/896	0.30/0.35	*0.29*/0.44	460/524	*0.19*, *0.23*; 0.32, 0.50
18	2.3/3.0	5.6/7.0	5215/3472	2.00/1.23	*2.91*/1.55	504/504	*0.23*, *0.50*; 0.25, 0.52
19	2.7/3.3	4.8/5.0	3593/3232	1.14/1.01	*2.36*/1.62	510/510	*0.25*, *0.50*; 0.22, 0.57
20	2.2/3.0	4.8/6.8	1845/1789	0.60/0.57	*1.22*/0.83	534/534	*0.33*, *0.55*; 0.33, 0.56

[a] Taken at a current density of 100 mA/cm^2.

(6.20 eV)[27] or Alq_3 (6.00 eV),[28] while the LUMO energy levels (1.86−2.40 eV) lie above those of TPBI (2.70 eV) or Alq_3 (3.30 eV). A range of average barriers exist for hole crossing and electron crossing at the carb/ETL interface, which would affect the luminance property and performance. In an attempt to use carb as both hole-transport and emitting materials, two types of double-layer EL devices were fabricated: (I) ITO/carb/TPBI/Mg:Ag; (II) ITO/carb/Alq_3/Mg:Ag. Bright emissions were obtained in all cases, with relatively low turn-on voltages and operating voltages, and electroluminescence data of the devices are shown in Table 2.

Shirota and co-workers reported the energetics between ITO and the hole-transport layer interface was critical to the operating voltage and the quantum efficiency of an OLED.[29] On the contrary, Forrest and co-workers found no correlationship between the HOMO energy and device quantum efficiency or turn-on voltage.[30] It is not certain whether the low turn-on voltages (I, 2.2−2.7 eV; II, 2.3−3.3 eV) and operating voltages at 100 mA/cm^2 (I, 4.8−6.5 eV; II, 4.2−7.0 eV) for both devices are due to the generally small energy difference between the work function of ITO and the HOMO levels of carb. It is known that in an ITO/NPD/Alq_3/Mg:Ag device, green emission from electron-transporting Alq_3 is obtained, whereas in the ITO/NPD/TPBI/Mg:Ag device, blue emission from the hole-transporting NPD is observed.[27c] The shifting of charge recombination zone in the latter case is due to a large barrier between the HOMOs of NPD and TPBI so that TPBI is serving as a hole blocker. Electrons cross into NPD layer instead, to give excitons of NPD. The energy level alignments for various carbazole devices are shown in Figure 3. In the type I devices with TPBI as ETL, emissions from the carb were observed for all derivatives examined, as suggested from a close resemblance of the EL and the PL of the corresponding carb. Furthermore, the recombination zone was found to be independent of the relative thickness of each individual layer. For instance, the EL spectra and efficiency for the three devices, **11** (300 Å)/TPBI (500 Å), **11** (400 Å)/TPBI (400 Å), and **11** (500 Å)/TPBI (300 Å), were found to be similar. This is reasonable by comparing the HOMO/LUMO levels of these compounds and that of TPBI. A much larger barrier exists for holes crossing from the HOMO

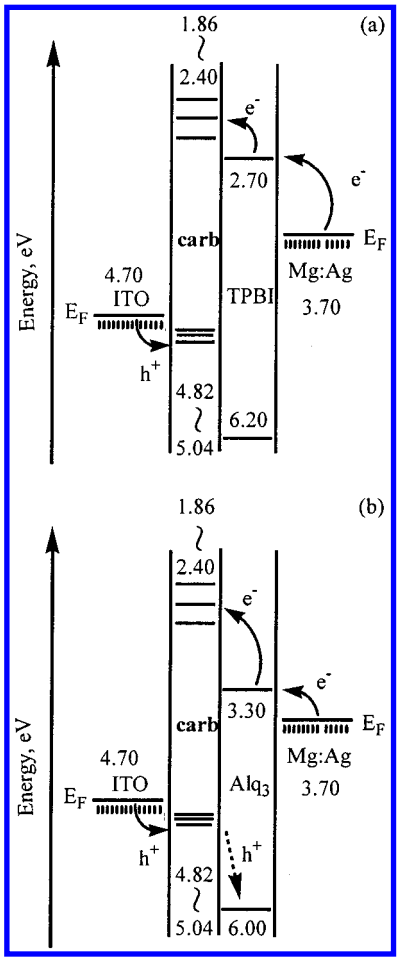

Figure 3. Relative energy alignments in ITO/carb/TPBI/Mg:Ag (a) and ITO/carb/Alq_3/Mg:Ag (b).

of carb to the HOMO of TPBI (1.2−1.4 eV) than for electrons crossing from the LUMO of TPBI to the LUMO of carb (0.55−0.75 e.V). In the type II devices with Alq_3 as ETL, again the emission from the carb layer was found for most cases *except* for **9**, **10**, **15**, and **16**, where characteristic green light of Alq_3 was observed. Some representative results are illustrated in Figure 4. In Figure 4a, the EL spectra for **20** are identical in both types of devices, giving a λ_{max} ~534 nm. Although this wavelength is close to that of Alq_3, emission from Alq_3 in the type II device is ruled out because of (1) the completely overlapping EL for type I and type II devices and (2) the clear deviation in peak position and bandwidth of our EL spectrum from those of the device known to give Alq_3 emission.[31] Similarly, in Figure 4b, the EL spectra for **18** are shown to be overlapping with each other. The λ_{max} of 504 nm agrees with

(27) (a) Zhang, X. H.; Lai, W. Y.; Gao, Z. Q.; Wong, T. C.; Lee, C. S.; Kwong, H. L.; Lee, S. T.; Wu, S. K. *Chem. Phys. Lett.* **2000**, *320*, 77. (b) Tao, Y. T.; Balasubramaniam, E.; Danel, A.; Tomasik, P. *Appl. Phys. Lett.* **2000**, *77*. 933. (c) Tao, Y. T.; Balasubramaniam, E.; Danel, A.; Jarosz, B.; Tomasik, P. *Appl. Phys. Lett.* **2000**, *77*. 1575. (d) Gao, Z. Q.; Lee, C. S.; Bello, I.; Lee, S. T.; Chen, R.-M.; Luh, T.-Y.; Shi, J.; Tang, C. W. *Appl. Phys. Lett.* **1999**, *74*, 865.

(28) Kwong, R. C.; Lamansky, S.; Thompson, M. E. *Adv. Mater.* **2000**, *12*, 1134.

(29) Giebeler, C.; Antoniadis, H.; Bradley, D. D. C.; Shirota, Y. *J. Appl. Phys.* **1999**, *85*, 608.

(30) O'Brien, D. F.; Burrow, P. E.; Forrest, S. R.; Koene, B. E.; Loy, D. E.; Thompson, M. E. *Adv. Mater.* **1998**, *10*, 1108.

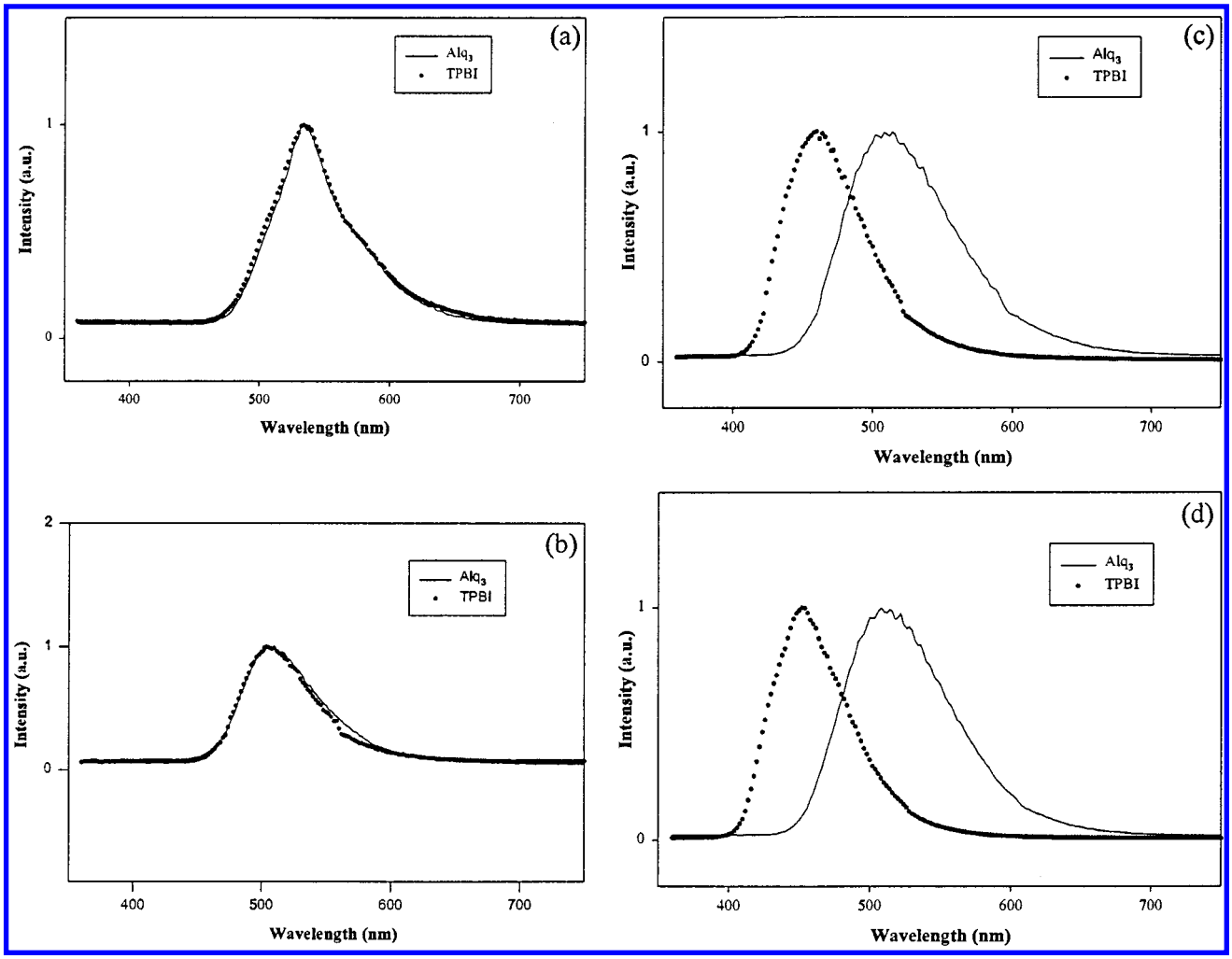

Figure 4. EL spectra the devices I and II for **20** (a), **18** (b), **9** (c), and **10** (d).

the PL of this compound but differs from that of Alq_3. Thus confinement of excitons in carb layer is suggested for both types of device. Panels c and d of Figure 4 show the EL of **9**- and **10**-based devices. A clear deviation of EL is seen, which suggests a different emitting zone for the two types of devices: carb for type I and Alq_3 for type II. These results can be understood from a delicate change in the relative barriers for holes crossing to Alq_3 and electrons crossing to carb. While the gaps between the HOMOs of these four carbs (**9**, **10**, **15**, and **16**) and that of Alq are not much different from other carb derivatives, these four compounds clearly have higher LUMO levels (1.86 e.V. to 2.07 e.V.) so that they effectively block the electrons from entering the carb layer. It is evident that the LUMO barrier (ΔE_{LUMO}) between carb and the hole blocking layer plays a dominating role on the EL efficiency and the current density of the devices. The correlation diagram of ΔE_{LUMO} versus external quantum efficiency or power efficiency (Figure 7a), and ΔE_{LUMO} versus current density (Figure 7b) for type I devices indicates that lowering ΔE_{LUMO} in general raises the EL efficiency and the current density of the device. With these devices, the recombination occurred in the HTL. A lower LUMO barrier is in favor of electron crossing to HTL and enhances recombination efficiency. Some deviation found may be attributed to the different carrier capability among different materials.

(31) In separate experiments, four devices were fabricated: (A) **11** (40 nm)/Alq_3 (40 nm); (B) **11** (40 nm)/BCP (10 nm)/Alq_3 (40 nm); (C) **11** (40 nm)/TPBI (40 nm); (D) NPD (10 nm)/Alq_3 (40 nm). Device D is the standard device in which light is emitted from the Alq_3 layer. The bandwidths for devices A−D are 78, 74, 74, and 96 nm, respectively.

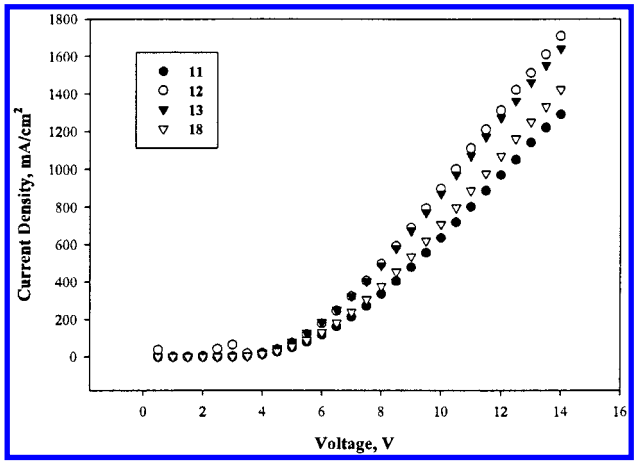

Figure 5. Current density vs applied electric field characteristics of the device ITO/carb/TPBI/Mg:Ag.

It is noteworthy that several devices of type I emit green light from carb with exceptional brightness even though the solution quantum efficiencies of these carbazole compounds do not exceed 0.2. Selective *I*−*V*−*L* characteristics are illustrated in Figures 5 and 6. While the device is not optimized, the physical performance appears to be promising: maximum luminescence (**12**, 38769 cd/m^2 at 13.5 V; **19**, 33961 cd/m^2 at 14.5 V; **11**, 41973 cd/m^2 at 14.0 V; **13**, 48853 cd/m^2 at 13.5 V; **14**, 33783 cd/m^2 at 14.5 V; **18**, 49326 cd/m^2 at 14.5 V;), maximum external quantum efficiency (**12**, 1.50% at 5 V; **19**, 1.27% at 3.5 V; **11**,

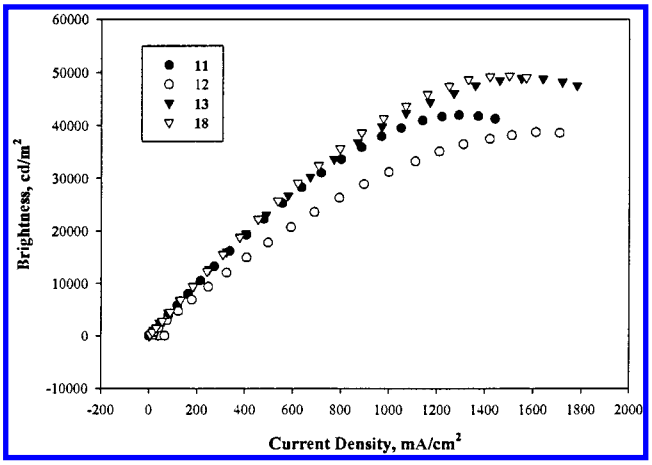

Figure 6. Luminance vs applied electric field characteristics of the device ITO/carb/TPBI/Mg:Ag.

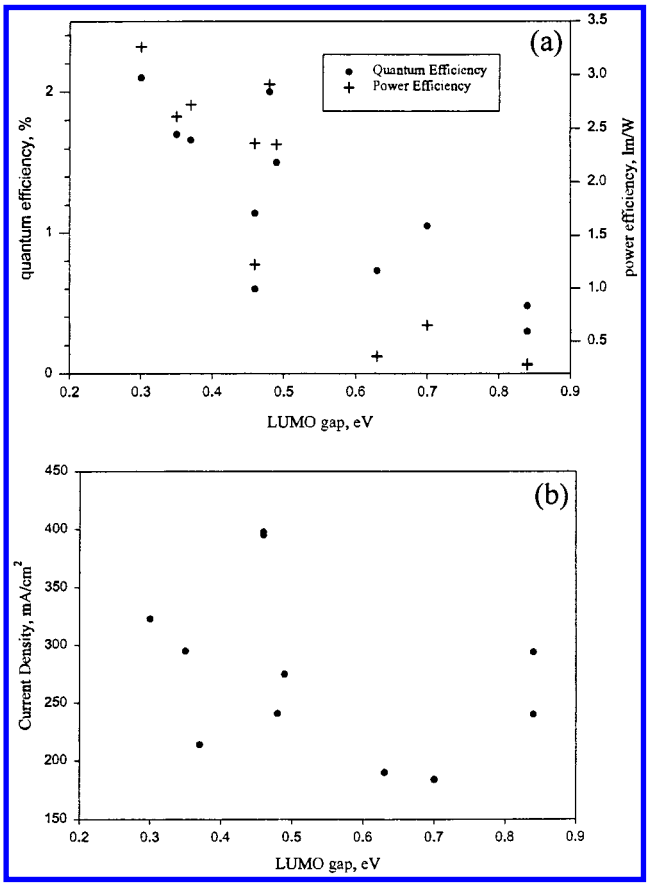

Figure 7. (a) EL efficiency vs LUMO barrierof carb/hole-blocking layer. (b) Current density (at 7.0 V applied voltage) vs LUMO barrier of carb/hole-blocking layer.

1.66% at 6.0 V; **13**, 2.19% at 4.0 V; **14**, 1.74% at 4.0 V; **18**, 2.00% at 5.5 V), and maximum luminous efficiency (**12**, 2.74 lm/W at 4.5 V; **19**, 2.90 lm/W at 3.5 V; **11**, 3.88 lm/W at 4.0 V; **13**, 4.77 lm/W at 3.5 V; **14**, 5.68 lm/W at 3.0 V; **18**, 4.12 lm/W at 3.5 V). These figures are in general better than those of typical green light-emitting devices based on the structure ITO/diamine/Alq_3/Mg:Ag under similar device structure.[32] A standard device of the structure ITO/α-NPD (500 Å)/Alq_3 (500 Å)/Mg:Ag was also fabricated for comparison and found to have external quantum efficiency at 1%, turn-on voltage at 5 V and maximum luminescence at 30 000 cd/m^2. On the contrary, only **19** and **14** have maximum luminescence in excess of 30 000 cd/m^2 (maximum luminescence, 33 961 cd/m^2 at 14.0 V for **19** and 33 306 cd/m^2 at 14.5 V for **14**; external quantum efficiency, 1.01% at 6.0 V for **19** and 1.42% at 6.0 V for **14**; luminous efficiency: 2.01 lm/W at 4.5 V for **19** and 2.38 lm/W at 5.0 V for **14**) among the type II devices where carbs are the emitters. It is interesting to note that the hole-transporting carbs serve as the emitting layer in most green light-emitting devices studied here, which is different from many standard green light-emitting devices where electron-transporting Alq_3 served as the emitting layer.

Another interesting feature of these carbazole compounds is that the luminescence wavelength can be tuned from green to blue through appropriate modifications of the structure, such as the change of the substituents at the peripheral nitrogen atom or the spacer between the peripheral nitrogen atom and the 3,6-carbon atoms of the central carbazole. The devices of type I fabricated from **9**, **10**, **15**, and **16** emit blue light (CIE (x, y): **9** (0.15, 0.14); **10** (0.15, 0.11); **15** (0.15, 0.12); **16** (0.19, 0.23)). The physical performance (maximum luminescence, 7802 cd/m^2 at 12.5 V for **9**, 5563 cd/m^2 at 14.0 V for **10**, 15 117 cd/m^2 at 14.0 V for **15**, and 2800 cd/m^2 at 12.0 V for **16**; external quantum efficiency, 1.10% at 7.0 V for **9**, 0.73% at 5.5 V for **10**, 0.48% at 5.5 V for **15**, and 0.25% at 5.5 V for **16**; luminous efficiency, 0.72 lm/W at 4.5 V for **9**, 0.57 lm/W at 3.5 V for **10**, 0.44 lm/W at 3.5 V for **15**, and 0.32 lm/W at 4.0 V for **16**) of these devices remains to be improved in comparison with some newly developed blue-emitting systems.[27b,d,33]

Devices based on these materials appear to be promising in terms of lifetime. In a preliminary study, parallel comparison of performances of devices **11**/Alq_3 and **13**/Alq_3 and the standard NPB/Alq_3 were made at a constant operating current of 5 mA for up to 120 h. Both carb-based devices exhibited slower decay in luminance and smaller increase in driving voltage than the standard device. This may be attributed to the higher T_g for the two materials used.

In summary, we have synthesized new carbazole-based hole-transporting molecules with high glass transition temperatures. Use of these amorphous materials as hole-transporting and emitting layer results in green- or blue-emitting LED devices with promising physical performance. Further modification of the molecules at the 3-, 6- and 9-positions of the carbazole aiming at color tuning and multiple functions (such as electron and hole transporting as well as emitting) is currently in progress.

Acknowledgment. We thank Academia Sinica and the National Science Council for supporting this work.

Supporting Information Available: Data for **4**, **8**−**11**, **13**, **14**, and **16**−**18**. This material is available free of charge via the Internet at http://pubs.acs.org.

JA010819S

(32) (a) Kido, J.; lizumi, Y. *Chem. Lett.* **1997**, 963. (b) Tang, C. W.; VanSlyke, S. A. *Appl. Phys. Lett.* **1987**, *51*, 913.

(33) (a) Leung, L. M.; Lo, W. Y.; So, S. K.; Choi, W. K. *J. Am. Chem. Soc.* **2000**, *122*, 5640. (b) Tao, X. T.; Suzuki, H.; Wada, T.; Miyata, S.; Sasabe, H. *J. Am. Chem. Soc.* **1999**, *121*, 9447. (c) Tamoto, N.; Adachi, C.; Nagai, K. *Chem. Mater.* **1997**, *9*, 1077. (d) Hosokawa, C.; Higashi, H.; Nakamura, H.; Kusumoto, T. *Appl. Phys. Lett.* **1995**, *67*, 3853.